3492–3502 *Nucleic Acids Research, 2005, Vol. 33, No. 11*
doi:10.1093/nar/gki659

Triplex-induced recombination and repair in the pyrimidine motif

Jennifer M. Kalish[1,2], Michael M. Seidman[3], Daniel L. Weeks[4] and Peter M. Glazer[1,2,*]

[1]Department of Therapeutic Radiology and [2]Department of Genetics, Yale University School of Medicine, PO Box 208040, HRT 140, New Haven, CT 06520-8040, USA, [3]National Institute on Aging, National Institutes of Health, 5600 Nathan Shock Drive, Baltimore, MD 21224, USA and [4]Department of Biochemistry, University of Iowa, Iowa City, IA 52242, USA

Received May 2, 2005; Revised and Accepted May 27, 2005

ABSTRACT

Triplex-forming oligonucleotides (TFOs) bind DNA in a sequence-specific manner at polypurine/polypyrimidine sites and mediate targeted genome modification. Triplexes are formed by either pyrimidine TFOs, which bind parallel to the purine strand of the duplex (pyrimidine, parallel motif), or purine TFOs, which bind in an anti-parallel orientation (purine, anti-parallel motif). Both purine and pyrimidine TFOs, when linked to psoralen, have been shown to direct psoralen adduct formation in cells, leading to mutagenesis or recombination. However, only purine TFOs have been shown to mediate genome modification without the need for a targeted DNA-adduct. In this work, we report the ability of a series of pyrimidine TFOs, with selected chemical modifications, to induce repair and recombination in two distinct episomal targets in mammalian cells in the absence of any DNA-reactive conjugate. We find that TFOs containing N3′P5′ phosphoramidate (amidate), 5-(1-propynyl)-2′-deoxyuridine (pdU), 2′-*O*-methylribose (2′-O-Me), 2′-*O*-(2-aminoethyl)-ribose, or 2′-*O*, 4′-C-methylene bridged or locked nucleic acid (LNA)-modified nucleotides show substantially increased formation of non-covalent triplexes under physiological conditions compared with unmodified DNA TFOs. However, of these modified TFOs, only the amidate and pdU-modified TFOs mediate induced recombination in cells and stimulate repair in cell extracts, at levels comparable to those seen with purine TFOs in similar assays. These results show that amidate and pdU-modified TFOs can be used as reagents to stimulate site-specific gene targeting without the need for conjugation to DNA-reactive molecules. By demonstrating the potential for induced repair and recombination with appropriately modified pyrimidine TFOs, this work expands the options available for triplex-mediated gene targeting.

INTRODUCTION

Triplex-forming oligonucleotides (TFOs) provide potential tools for altering gene function by either repressing transcription, inhibiting DNA replication or inducing site-specific mutagenesis and recombination (1–6). TFOs bind in the major groove of DNA in a sequence-specific manner to polypurine/polypyrimidine sequences, in two distinct motifs (7–10). TFOs in the purine motif bind anti-parallel to the purine strand of the duplex via reverse-Hoogsteen hydrogen bonds and TFOs in the pyrimidine motif bind in a parallel orientation via Hoogsteen bonds (7–10). The third-strand binding code specifies that in the purine motif G and A in the third strand bind to the duplex G and A, respectively; while in the pyrimidine motif C and T bind to the duplex G and A, respectively (11).

Binding affinity in the two motifs is differentially affected by pH and ion concentrations. In the pyrimidine motif, the need for protonation of cytosines at the N3 position (favored at low pH) limits the binding affinity of TFOs composed of unmodified DNA under physiological conditions (12). In order to make TFOs more effective tools, chemical modifications have been developed to enhance third-strand binding under *in vivo* conditions. Base modifications such as 5-methyl-2′-deoxycytidine (5meC) and 5-methyl-2′-deoxyuridine (pdU) and sugar modifications such as 2′-*O*-(2-aminoethyl)-ribose (2′-AE) substitution improve binding affinity and psoralen delivery in the pyrimidine motif (13,14). Pyrimidine TFOs with an amidate backbone (in which nitrogen replaces the bridging 3′ oxygen of the diester) have also been shown to form stable triplexes at neutral pH (15).

*To whom correspondence should be addressed. Tel: +1 203 737 2788; Fax: +1 203 785 6309; Email: peter.glazer@yale.edu

In addition, conjugation of intercalators such as pyrene and acridine to TFOs has been shown to further increase their biological activity (16). Although purine TFOs consisting of standard DNA [except for 3′ end-capping (4,17)] have been shown to be active in cells and animals (16–18), fewer strategies have been established for effective modification of purine TFOs. The most effective option that has been demonstrated is backbone substitution with *N*,*N*-diethylethylenediamine (DEED) internucleoside linkages which reduce the Mg^{2+}-dependence and enhance intracellular activity of polypurine TFOs (18).

Both purine and appropriately modified pyrimidine TFOs have been used to direct psoralen intercalation and photoadduct formation to specific sites in mammalian cells and yeast (16,17,19). In the absence of psoralen, however, only purine TFOs have been shown to induce genomic changes (either mutagenesis or recombination) via the effects of third-strand binding alone (4). Previous work has demonstrated that non-covalent triplexes formed by purine TFOs are active in stimulating repair and recombination in cell extracts, in cell culture and even in mice (3,5,20,21). Studies in human cell extracts and in DNA repair-deficient human cell lines have revealed the ability of non-covalent purine motif triplexes to provoke recombination in a manner dependent on the nucleotide excision repair (NER) pathway (4). However, the ability of non-covalent triplexes formed by pyrimidine TFOs to induce recombination has not been established.

In the work reported here, we sought to determine the extent to which triplexes formed by pyrimidine TFOs can stimulate recombination and repair. Because standard DNA TFOs bind poorly in the pyrimidine motif, we evaluated TFOs containing a series of modifications to determine which, if any, are effective in provoking DNA metabolism via third-strand binding alone, in the absence of a DNA-reactive conjugate. Interestingly, although several modifications did support high-affinity binding under physiological conditions *in vitro*, only amidate and pdU-modified TFOs induced recombination in episomal targets in cells and repair in cell extracts. These results demonstrate that certain pyrimidine TFOs can provoke recombination without the need for covalent damage to the DNA. Because pyrimidine triplexes are favored at A:T bp-rich sites (in contrast to purine triplexes, which are favored at G:C-rich sites), these findings increase the number of potential genomic target sites suitable for modification by non-covalent triplexes. In addition, we propose a model in which TFO sugar substitution at the 2′ position may influence the extent to which the resulting triplex can provoke DNA metabolism, with reference to NMR studies showing that 2′ substitution of the TFO influences the degree of structural distortion of the duplex to which the TFO is bound (22).

MATERIALS AND METHODS

Oligonucleotides and vectors

Oligonucleotides were obtained from Transgenomic (amidate18), Gilead Sciences and Eurogentec (G3pUmC18), Oligos Etc. (G3TmC18, 2′-O-Me18), Proligo (LNA18, LNAcontrol) and Eurogentec (LNA18, UmCcontrol), Gene Tools (morph18), Midland Certified Reagents Company (AG30, SCR30, MIX30, Fluc13) and Keck Oligonucleotide Synthesis Facility (Yale University) (AG19, DNA18). Duplex target oligonucleotides (G3Y, G3R) were synthesized by Oligos Etc. When the chemical modification did not provide protection against exonuclease degradation, which is necessary for cell targeting experiments, 3′ ends were synthesized to contain a 3′ propylamine group, using the C3 amino-CPG from Glen Research. The following oligonucleotides contain a 3′ propylamine group: G3TmC18, G3pUmC18, AG30, SCR30 and MIX30. Three terminal phosphorothioate linkages were synthesized on the 3′ end of 2′-O-Me18 and Fluc13 has terminal phosphothioate linkages on both ends. Pyrimidine TFO sequences and modifications are listed in Figure 1. The sequences for the control oligonucleotides are as follows: AG30, 5′-AGGAAGGGGGGGGTGGTGGGGGAGGGGGAG-3′; SCR30, 5′-′GGAGGAGTGGAGGGGAGTGAGGGGGGGGGG-3′; MIX30, 5′-AGTCAGTCAGTCAGTCAGTCAGTCAGTCAG-3′; Fluc13, 5′-TGGTAAAGCCACCATGGAAGACGCCAAAAACATAAAGAAAGGCCCGGCGCC-3′; UmCcontrol, 5′-cucucucucuuuuuuu-3′ (c = 5meC, u = pdU); LNAcontrol, 5′-TtTTCtTTTtTCTtTTCt-3′ (t = LNA); AG19, 5′-AGGAAGGGGGGGGTGGTGGG-3′; DNA18, 5′-TTTTCTTTTTTCTTTTCT-3′.

The pSupFTC18 shuttle vector, derived from pSP189 (23), carries two copies of the *supF* gene, each with a distinct mutation, flanking an 18-bp A-rich homopurine/homopyrimidine target site [the TC18 site from pLSG3 (13)]. These mutations were created using the QuikChange Site-Directed Mutagenesis Kit (Stratagene). These mutations result in inactive tRNAs which lack the ability to suppress the amber mutation in the *lacZ* gene in MBM7070 *Escherichia coli* which are used as indicator hosts for this recombination assay (24).

The plucTC18 vector was derived from a plasmid constructed by subcloning the firefly luciferase gene *Fluc*+ (pGL3-Basic Vector; Promega) into pcDNA5/FRT (Invitrogen) (25). The TC18 target site was inserted 40 bp upstream of the *Fluc*+ start site. Site-specific mutagenesis was used to create a stop codon at bp 13 downstream from the start codon.

The pRLTC18 vector was constructed by adding the TFO target site [the TC18 site from pLSG3 (13)] into the multiple cloning region of the pRL-CMV vector (Promega).

Third-strand binding assays

Third-strand binding was measured using gel mobility shift assays under native conditions. Two complementary 30mers (G3Y, G3R) containing the TC18 target from pLSG3 (representing bp 76–105) were synthesized. Duplex DNA was prepared by mixing 1000 pmol of each 30mer together with 50 mM NaCl and incubating at 85°C for 20 min and cooling to room temperature before end-labeling with T4 polynucleotide kinase (New England BioLabs) and [γ-^{32}P]ATP (Amersham Biosciences). Duplex was gel purified, electroeluted and filtered by Centricon (Millipore). A fixed concentration of duplex at 5×10^{-8} M was added to binding reactions with increasing concentrations of oligonucleotides in 20 µl of 10 mM Tris (pH 7.2) and selected concentrations of $MgCl_2$ (0.1 or 10 mM) and KCl (0 or 140 mM). Binding for full DEED18 was carried out at pH 7.6 with the addition of 1 mM spermine. Binding assays were also carried out at pH 5.4, in which case 40 mM Tris–acetic acid was substituted

A

Duplex target and oligonucleotides

```
     G3Y 5'tcgaggTCTTTTCTTTTTTCTTTTagggggg3'
     G3R 3'agctccAGAAAAGAAAAAAGAAAAtccccccc5'

amidate18      3' tcttttctttttctttt 5'
pDEED18        3' TcTTTTcTTTTTtCTTTt 5'
full DEED18    3' tcttttctttttctttt 5'
G3TmC18        3' TcTTTTcTTTTTTcTTTT 5'
G3pUmC18       3' ucuuuucuuuuuucuuuu 5'
LNA18          3' TcTtTtCtTtTtTcTtTt 5'
2'-O-Me18      3' tcttttctttttctttt 5'
2'-AE18        3' UcuuuUCUUUUUUCUUUU 5'
morph18        3' tcttttctttttctttt 5'
```

B

Chemical Structures

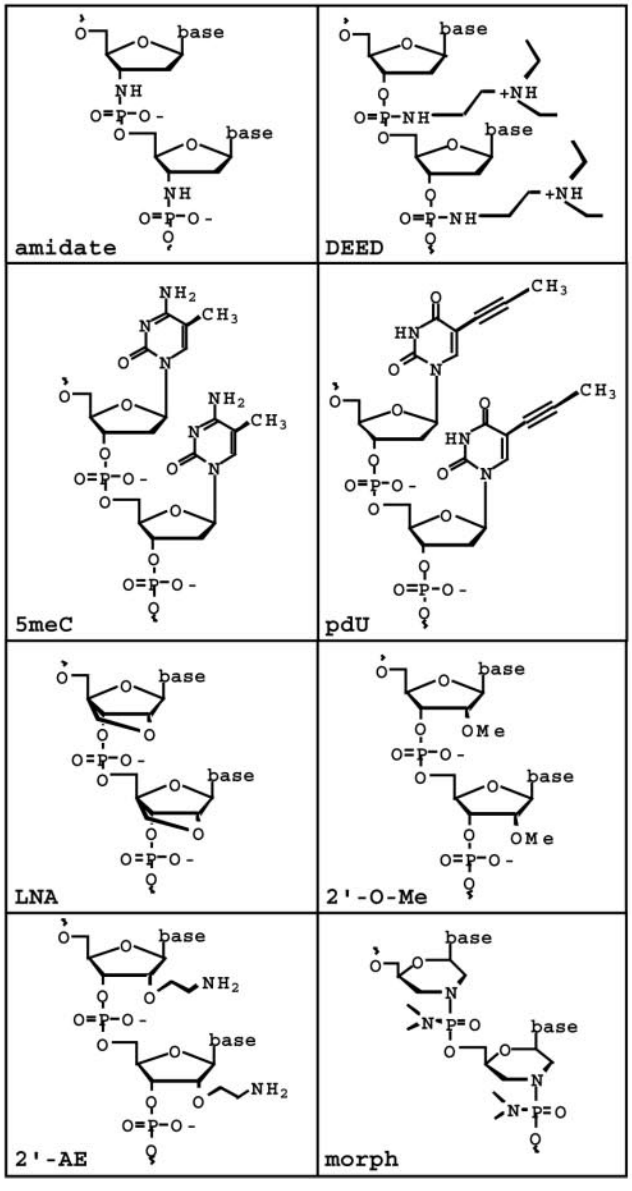

for Tris base at pH 5.4. Samples were incubated at 37°C for 16 h unless otherwise specified.

Samples bound at pH 7.2 were loaded onto 15% polyacrylamide gels [acrylamide/bisacrylamide (19:1)] containing 17.8 mM Tris and 17.8 mM boric acid (pH 7.2) and 10 mM $MgCl_2$ and the gels were run in the same concentration of Tris-boric acid and $MgCl_2$ at 60 V for 6 h at 23°C. For samples bound at pH 5.4, 15% polyacrylamide gels containing 40 mM Tris–acetate and 10 mM $MgCl_2$ were used and gels were run in buffers of the same concentration of Tris–acetate and $MgCl_2$ at 60 V for 6 h at 23°C.

Shuttle vector recombination assay

Monkey COS-7 cells were obtained from ATCC (1651-CRL) and grown in DMEM/10% fetal bovine serum (FBS) (Gibco). Cells were grown to 50–70% confluency and cell transfection was performed with GenePORTER2 (Gene Therapy Systems, Inc.). Cells were transfected with 1 μg of pSupFTC18 followed 24 h later by a second, separate transfection with 1 μg of oligonucleotide. Cells were harvested at 48 h after oligonucleotide transfection and shuttle vector DNA was isolated by a modified alkaline lysis procedure, as described previously (6). Vector samples were used to transform indicator bacteria [MBM7070 [lacZ(Am)] (23)] by electroporation (Bio-Rad; settings 25 μF, 250 W and 1800 V; 0.1 cm electrode gap cuvette), and colonies were screened for supF function by growth on plates supplemented with 75 μg/ml ampicillin, 210 μg/ml X-Gal and 200 μg/ml isopropyl-β-D-thiogalactopyranoside. Recombination events were indicated by wild-type blue colonies in a background of white colonies.

Chinese hamster ovary (CHO) cell transfection and luciferase assay

CHO cells were obtained from Invitrogen and grown in F12/10% FBS (Gibco) supplemented with 2 mM L-glutamine (Gibco) and 100 μg/ml Zeocin (Invitrogen). CHO cells were transfected and the luciferase activity was assayed as described previously (25). Briefly, 24 h prior to transfection, 12-well plates were seeded with 5×10^4 cells/well. plucTC18 was preincubated overnight with Fluc13 (an oligonucleotide containing the wild-type luciferase sequence for the mutated

Figure 1. Oligonucleotide sequences and chemical structures. (**A**) Duplex target and oligonucleotide modifications. The third-strand binding site is indicated in upper case letters in the duplex (G3Y/G3R) used for binding studies. For the oligonucleotides, lower case letters indicate modified nucleotides with the specific chemistry as indicated in the name of the oligonucleotide. Upper case letters indicate unmodified nucleotides. All internucleoside linkages in amidate18 are N3′→P5′ phosphoramidate (amidate)-modified. DEED-modified nucleotides are present in partial DEED (pDEED18) and full DEED18 as indicated. G3TmC18 contains 5-methyl-2′-deoxycytidines (5meC) in place of cytidines. G3pUmC18 contains 5meC-modifications on all cytidines and all thymines are replaced by pdU. LNA18 contains unmodified nucleotides alternating with 2′-O, 4′-C-methylene bridged or LNA-modified nucleotides. 2′-O-Me18 contains 2′-O-Me-modified nucleotides and all cytidines have 5meC-modifications. 2′-AE18 contains 2′-AE-modified nucleotides at the four lower case letter positions, while the upper case positions have 2′-O-Me modifications and all positions also have either 5meC-modifications or 5-methyl-2′-deoxyuridine modifications. All nucleotides in morph18 are morpholino (morph)-modified. (**B**) Structures of the chemical modifications. N3′→P5′ phosphoramidate (amidate); *N*,*N*-diethylethylenediamine (DEED); 5-methyl-2′-deoxycytidine (5meC); 5-(1-propynyl)-2′-deoxyuridine (pdU); 2′-*O*,4′-*C*-methylene bridged or locked nucleic acid (LNA); 2′-*O*-methyl-ribose (2′-O-Me); 2′-*O*-(2-aminoethyl)-ribose (2′-AE); morpholino (morph).

region) and the TFO to be tested with 10 mM $MgCl_2$ and 10 mM Tris (pH 7.2) at 37°C. Cells were transfected with GenePORTER2 as described above. Each transfection delivered 0.3 μg of plasmid, donor and TFO per well. Cells were collected 48 h post-transfection by rinsing twice with PBS followed by lysis with 1× Passive Lysis Buffer (Promega). Luciferase activity was measured using the Promega Dual Luciferase Kit and only the LAR II substrate. The total protein in the cell lysate was determined via Bradford protein assay (26).

In vitro repair synthesis assay

Repair reactions were carried out as described previously (27), with several modifications. HeLaScribe Nuclear Extract *in vitro* Transcription Grade (Promega) was used. The pRLTC18 plasmid (500 ng) containing the TC18 target sequence was preincubated with 1 μM TFO (37°C, 18 h, 10 mM Tris, pH 7.2 and 10 mM $MgCl_2$). As a positive control, one sample was incubated with sterile water in place of oligonucleotide, this sample was then damaged by UVC radiation treatment (2 inches, 30 s). The DNA was added to HeLa cell-free extracts with [α-^{32}P]dCTP and supplemented as described previously (27). Samples were incubated for 3 h at 30°C and the reactions were stopped as previously described (27). Substrate plasmid DNAs were isolated from the reaction by phenol/chloroform/iso-amyl alcohol extraction and EtOH precipitation. The isolated vector DNAs were linearized by XhoI digestion and the samples were analyzed by gel electrophoresis. DNA repair synthesis was quantified by measuring [α-^{32}P]dCTP incorporation using a phosphorimager (Storm 860; Molecular Dynamics, Amersham Pharmacia Biotech). The quantified value of the UVC-treated sample was set to 100% and used to normalize the measurements of the other samples.

Shuttle vector assay in repair-deficient and corrected cells

XP12BE cells (deficient in the NER factor, XPA) were obtained from Coriell Cell Repositories (GM04429) and grown in MEM/10% FBS (Gibco). The shuttle vector recombination assay was performed as described above except that, in some cases, the cells were also transfected with 1 μg of a plasmid containing XPA cDNA [XPA cDNA with a His tag on the C-terminus cloned into the multiple cloning site of pcDNA3.1 (Invitrogen)] at the same time the cells were transfected with the pSupFTC18. XPA expression was verified by western blot. Briefly, cells were lysed (at 48 and 72 h post-transfection) with RIPA buffer (150 mM NaCl and 0.1% SDS) and 100 μg of total protein per sample was resolved on 12% SDS–PAGE gels. Proteins were detected by standard immunoblot procedures using XPA (28) and tubulin (clone B-5-1-2; Sigma) primary antibodies.

Serum stability assay

Each oligonucleotide was 5′ end-labeled at a concentration of 1 μM with [γ-^{32}P]ATP (Amersham) using T4 polynucleotide kinase (New England BioLabs) for 1 h, followed by heat inactivation for 20 min at 70°C. An aliquot of 5 μl of end-labeled oligonucleotide was added to 100 μl of FBS (Gibco) and incubated at 37°C. Aliquots were removed at 0–24 h and added to an equal volume of formamide dye, before being run on a 20% denaturing polyacrylamide gel. Visualization and quantification of intact oligonucleotide was performed using a phosphorimager.

RESULTS

TFO target site and oligonucleotide modifications

To examine the ability of triplexes formed in the pyrimidine, parallel motif to induce recombination and repair, we evaluated a series of chemically modified pyrimidine TFOs each designed to bind to an 18 bp A-rich duplex target site (Figure 1). The modifications included amidate and DEED internucleoside linkages and 5meC and pdU base substitutions. Sugar modifications included LNA, 2′-O-Me and 2′-AE substitutions. Morpholino TFOs consist of both sugar and backbone changes (Figure 1).

We chose these modifications because either they have been shown to enhance intracellular delivery of psoralen conjugates to target genes [amidate (29–33), DEED (18), 5meC (13,34), pdU (13,34,35), 2′-O-Me (14) and 2′-AE (14)] or they have been found to provide enhanced third-strand binding *in vitro* [LNA (36–38) and morpholino (39,40)]. In the case of the DEED modification, enhanced chromosome targeting has been demonstrated only in the purine motif. However, the ability of the DEED internucleoside substitution to confer a potentially advantageous positive charge on the TFO prompted us to consider pyrimidine TFOs with either full or partial DEED modifications.

Unless otherwise specified, all TFOs contained phosphodiester backbones. In some cases, all nucleotides were modified in a given TFO while in other cases only selected ones were modified, as indicated (Figure 1). The C residues in G3TmC18, G3pUmC18, 2′-O-Me18 and 2′-AE18 were substituted with 5meC, because this modification has been shown to enhance third-strand binding at physiological pH (41,42). Nucleotides in 2′-AE18 not containing the 2′-AE modification were synthesized to contain 2′-O-Me modifications.

In vitro binding measurements

The binding affinities of TFOs with the modifications described above were compared under a series of conditions as determined by gel mobility shift assays in non-denaturing gels. Binding was quantified and equilibrium dissociation constants (K_d, representing TFO concentrations yielding half-maximal binding) were determined. Because stable triplex formation is dependent on Mg^{2+} and sensitive to K^+ (43,44), we tested binding in either 0.1 or 10 mM $MgCl_2$ and either 0 or 140 mM KCl (both conditions at pH 7.2). In recognition of the possible pH dependence of binding by certain TFOs, we also tested binding at pH 5.4 (in 10 mM $MgCl_2$ and without KCl).

Under conditions where the minimally modified TFO, G3TmC18, formed triplexes (pH 5.4, 10 mM $MgCl_2$ and 0 mM KCl), all of the chemically modified TFOs formed triplexes (Figure 2). However, there was a range of binding affinities (Figure 2 and Table 1). The best binding was seen with the amidate, LNA, 2′-AE, pdU and 2′-O-Me-modified oligonucleotides, with K_d values of 2.8×10^{-10}, 3.0×10^{-10},

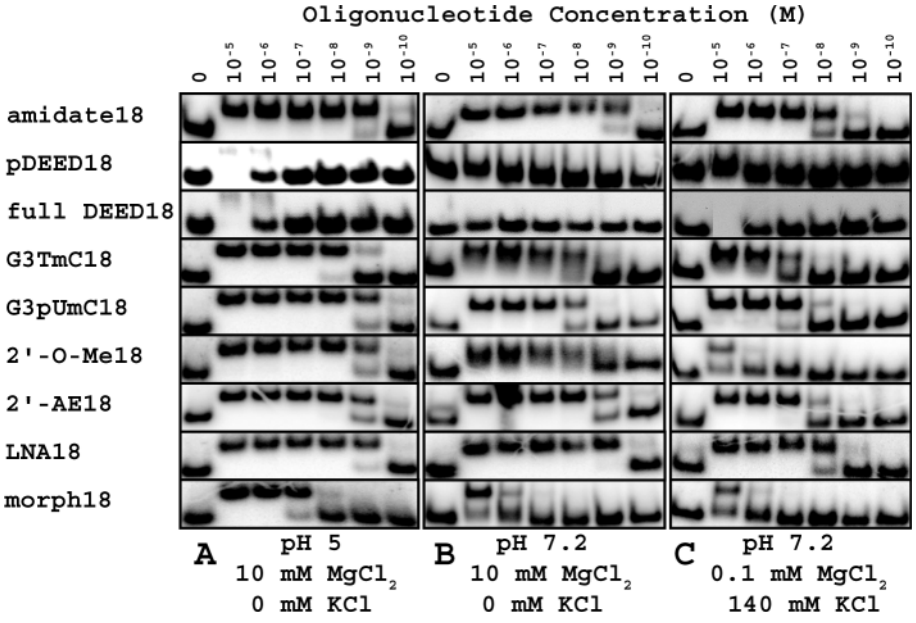

Figure 2. Third-strand binding under selected conditions as determined by gel mobility shift analysis. The first lane in each panel contains duplex alone (0 concentration of TFO), the second lane contains 10^{-5} M oligonucleotide, and each subsequent column contains a 10-fold dilution. Third-strand binding conditions: (**A**) pH 5.4, 10 mM $MgCl_2$ and 0 mM KCl; (**B**) pH 7.2, 10 mM $MgCl_2$ and 0 mM KCl; (**C**) pH 7.2, 0.1 mM $MgCl_2$ and 140 mM KCl. The bands of reduced mobility relative to the duplex alone represent triplex formation.

Table 1. Binding of chemically modified pyrimidine oligonucleotides to an 18 bp A-rich site[a]

Oligonucleotide	pH 5.4 (10 mM $MgCl_2$ and 0 mM KCl)	pH 7.2 (10 mM $MgCl_2$ and 0 mM KCl)	pH 7.2 (0.1 mM $MgCl_2$ and 140 mM KCl)
amidate18	2.8×10^{-10}	8.0×10^{-10}	1.0×10^{-8}
pDEED18	3.0×10^{-8}	None	None
full DEED18	1.0×10^{-6}	None[b]	None
G3TmC18	3.0×10^{-9}	7.0×10^{-9}	3.0×10^{-7}
G3pUmC18	4.5×10^{-10}	7.0×10^{-9}	9.0×10^{-8}
2′-O-Me18	4.6×10^{-10}	1.5×10^{-10}	8.0×10^{-6}
2′-AE18	4.0×10^{-10}	6.0×10^{-10}	2.0×10^{-8}
LNA18	3.0×10^{-10}	2.7×10^{-10}	2.5×10^{-8}
morph18[c]	3.0×10^{-8}	3.5×10^{-6}	5.1×10^{-6}

[a]Binding affinities were calculated as equilibrium dissociation constants (K_d) under the indicated conditions as determined by gel mobility shift assay under non-denaturing conditions. K_d values are given in molarity. Binding was done for 16 h at 37°C unless otherwise specified.
[b]Binding was carried out at pH 7.6 with 1 mM spermine.
[c]Binding was performed at 23°C.

4×10^{-10}, 4.5×10^{-10} and 4.6×10^{-10} M, respectively (Figure 2 and Table 1). G3TmC18, morph18 and partially modified DEED oligonucleotides showed lower binding affinities, and the full DEED18 showed the lowest binding (Figure 2 and Table 1).

At neutral pH with 10 mM $MgCl_2$, the 2′-O-Me, LNA, 2′-AE and amidate-modified TFOs showed strong binding with K_d values of 1.5×10^{-10}, 2.7×10^{-10}, 6.0×10^{-10} and 8.0×10^{-10} M, respectively (Figure 2 and Table 1). The pdU and 5meC-modified TFOs showed ~10-fold weaker binding and the morpholino-modified TFO showed 1000-fold weaker binding. Neither of the DEED-modified oligonucleotides (partial or full) showed any binding at neutral pH.

Under physiological conditions (pH 7.2, 0.1 mM $MgCl_2$ and 140 mM KCl), the amidate, 2′-AE, LNA and pdU-modified TFOs showed the strongest binding with K_d values of 1.0×10^{-8}, 2.0×10^{-8}, 2.5×10^{-8} and 9.0×10^{-8} M, respectively. G3TmC18 showed slightly weaker binding, and the morpholino and the 2′-O-Me-modified TFO showed even weaker binding. The DEED-modified TFOs showed no detectable binding under these conditions.

TFO-induced recombination in COS-7 cells

To test triplex-induced recombination by pyrimidine TFOs, we constructed an SV40-based shuttle vector similar to pSupFAR used in previous work to test purine TFOs (20). However, in this case, we designed the vector to contain the 18 bp A-rich target site used in the binding assays above. This site is inserted between two copies of the *supF* gene, each with an inactivating point mutation, at bp 163 in the upstream gene and at bp 115 in the downstream gene (Figure 3A). The 5′ mutation is 33 bp from the beginning of the TFO binding site, while the 3′ mutation is 24 bp away from the end of the site. Recombination between the two genes can generate a functional *supF* gene, which can be scored upon shuttle vector transformation into indicator bacteria following vector DNA rescue from the COS-7 cells.

The plasmid vector was pre-transfected into the COS-7 cells to establish the episomal target in these cells. One day later, the cells were transfected with the TFOs and maintained in culture for 48 h to allow for triplex formation and possible induced recombination. As a negative control to establish the background frequency of recombination in this assay, we included in each experiment cells transfected with vector but mock-transfected the next day without TFO. The vector DNAs were harvested from the cells and analyzed for recombination

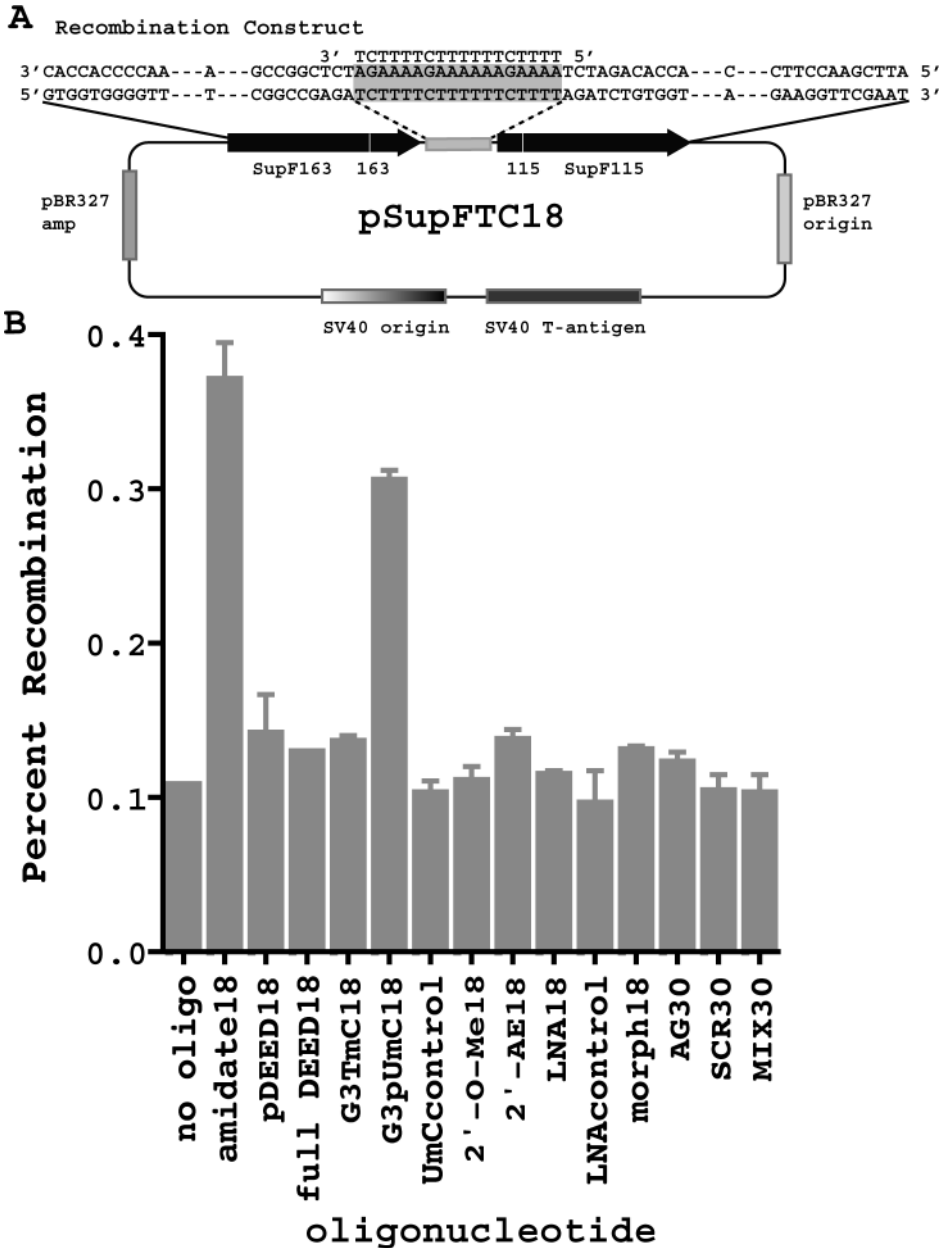

Figure 3. Induced recombination mediated by pyrimidine TFOs. (**A**) Schematic representation of the pSupFTC18 vector. This SV40-based vector contains two mutant *supF* genes in tandem. The upstream mutant *supF* gene, *supF163*, contains a C-to-T point mutation at nucleotide position 163. The downstream mutant *supF* gene, *supF115*, contains a G-to-A point mutation at nucleotide position 115. In between the two mutant *supF* genes is an 18 bp A–T-rich homopurine/homopyrimidine target site. The chemically modified oligonucleotides described in Figure 1A were designed to bind to this target sequence. (**B**) Triplex-induced recombination in COS-7 cells. The plasmid described in (**A**) was pre-transfected into COS-7 cells followed 1 day later by transfection of the indicated oligonucleotides or mock transfection. After 48 h, shuttle vector DNA was isolated and transformed into indicator bacteria to analyze *supF* gene function and allow quantification of recombination events. Percent recombination was calculated by the ratio of the number of blue colonies to total colonies.

events (Figure 3B). The results were normalized between experiments by comparison to the plasmid only (no oligonucleotide) background and presented as recombination frequency. Transfection of cells with the amidate18 and G3pUmC18 TFOs gave the highest levels of induced recombination, at 0.37 and 0.31%, respectively; whereas G3TmC18, 2′-AE18 and morph18 gave lower frequencies of 0.14, 0.14 and 0.13%, respectively. The 2′-O-Me, LNA and DEED TFOs had minimal effects over background. The control TFOs, UmCcontrol, LNAcontrol, AG30, SCR30 and MIX30 showed little effect over background.

To further control for sequence specificity, we tested induced recombination by the amidate18 and G3pUmC18 TFOs using a different shuttle vector, pSupFAR, as a target in the cells. pSupFAR contains two mutant *supF* genes flanking a 30 bp G-rich polypurine target site suitable for triplex formation in the purine motif (3). In previous work, we have shown that a G-rich TFO, AG30, can bind with high affinity to

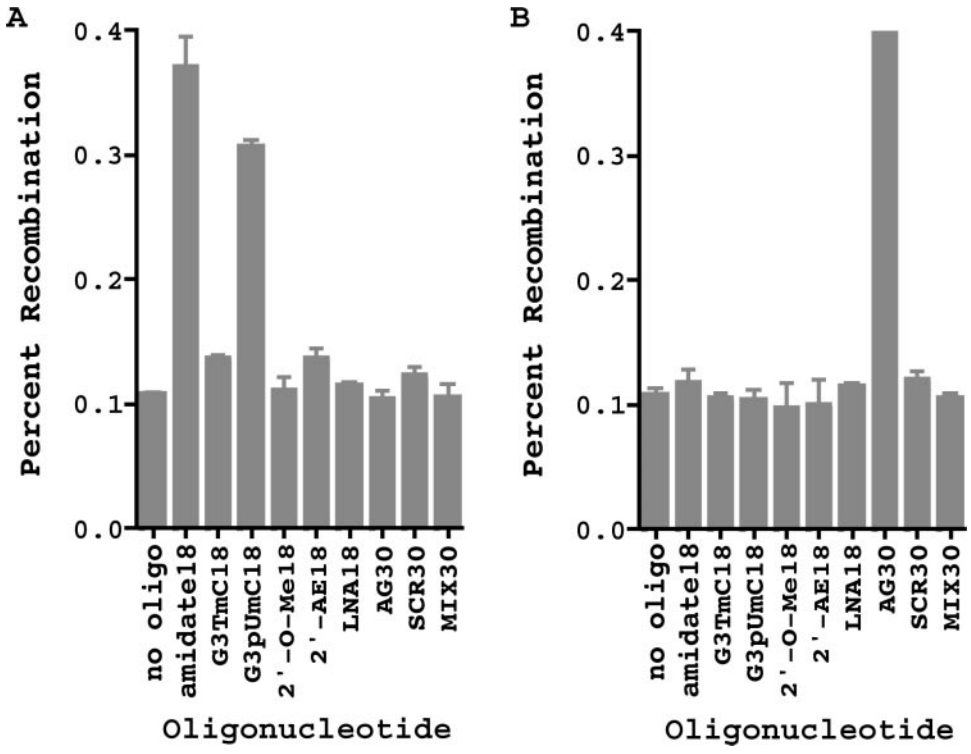

Figure 4. Sequence-specificity of the TFO-induced recombination. (**A**) Triplex-induced recombination with a pyrimidine motif target. Cells pre-transfected with the dual *supF* plasmid containing the 18 bp A–T-rich site, pSupFTC18, were transfected the next day with lipid reagent alone or with the indicated TFOs. AG30 and SCR30 are G-rich TFOs and MIX30 has a mixed sequence. Shuttle vector rescue and analysis were performed as for Figure 3. (**B**) Triplex-induced recombination with a purine motif target. Cells pre-transfected with a dual *supF* plasmid containing a 30 bp G-rich site, pSupFAR, were transfected 1 day later with lipid reagent alone or with the indicated TFOs. Analysis of recombination events was performed as above. Amidate18 and G3pUmC18 bind with high affinity to the A-rich target site in the intergenic region in pSupFTC18 but not to the G-rich site in pSupFAR. AG30 binds well to the site in pSupFAR but not to that in pSupFTC18.

the third-strand binding site in pSupFAR (3). AG30 shows no detectable binding to the A-rich polypurine site found in pSupFTC18; conversely, TC-rich pyrimidine TFOs show no binding to the G-rich site in pSupFAR (data not shown). We found that while transfection of amidate18 and G3pUmC18 into COS-7 cells can induce recombination in pSupFTC18, neither has an effect on recombination in pSupFAR in the same cell assay (nor do any of the other modified pyrimidine TFOs tested) (Figure 4). In contrast, AG30 can induce recombination in pSupFAR in COS-7 cells but has no effect on recombination in pSupFTC18 (Figure 4). Hence, the effects of the amidate18, G3pUmC18 and AG30 TFOs are sequence-specific, based on both oligonucleotide and target site controls.

TFO-induced recombination in CHO cells

To test pyrimidine-induced recombination in a different episomal target, we constructed the plucTC18 plasmid, which is a vector containing a pyrimidine TFO target adjacent to a mutated luciferase reporter gene, similar to a vector used in previous work studying targeting in the purine motif (25). The TFO binding site is 40 bp upstream from the start site of the luciferase gene, and a nonsense mutation that inactivates the luciferase gene is 13 bp downstream from the start site. In this assay, recombination induced by TFO binding occurs between the plasmid and a separate donor oligonucleotide (a 50mer) containing the wild-type luciferase sequence in the region of the mutation. The amidate18 was found to induce recombination at a frequency of 0.11% (Figure 5B), whereas the 2′-O-Me- and 2′-AE-modified TFOs showed minimal levels of induced recombination above background.

Pyrimidine TFO-induced repair in HeLa cell extracts

Because previous work had shown a correlation between the ability of purine TFOs to induce recombination and the ability of the triplexes they form to induce repair, we assayed for induced repair synthesis in HeLa cell-free extracts on plasmid substrates containing pyrimidine motif triplexes. The substrate for DNA repair was a plasmid incubated in the presence or absence of TFO. The amount of DNA repair-associated synthesis was measured based on the level of incorporation of [α-^{32}P]dCTP into the plasmid. This is a well-established assay for measuring repair provoked by a variety of DNA lesions (45–47). Amidate18 and G3pUmC18 showed the highest level of induced repair activity at 42 and 66%, respectively, as compared with UVC damage set at 100% activity (Figure 6A and B). G3TmC18 and LNA18 produced lower repair activity (Figure 6A and B).

Role of NER in induced recombination by pyrimidine TFOs

To determine if the induced recombination in cells by the amidate18 TFO is due to the NER pathway, a shuttle vector

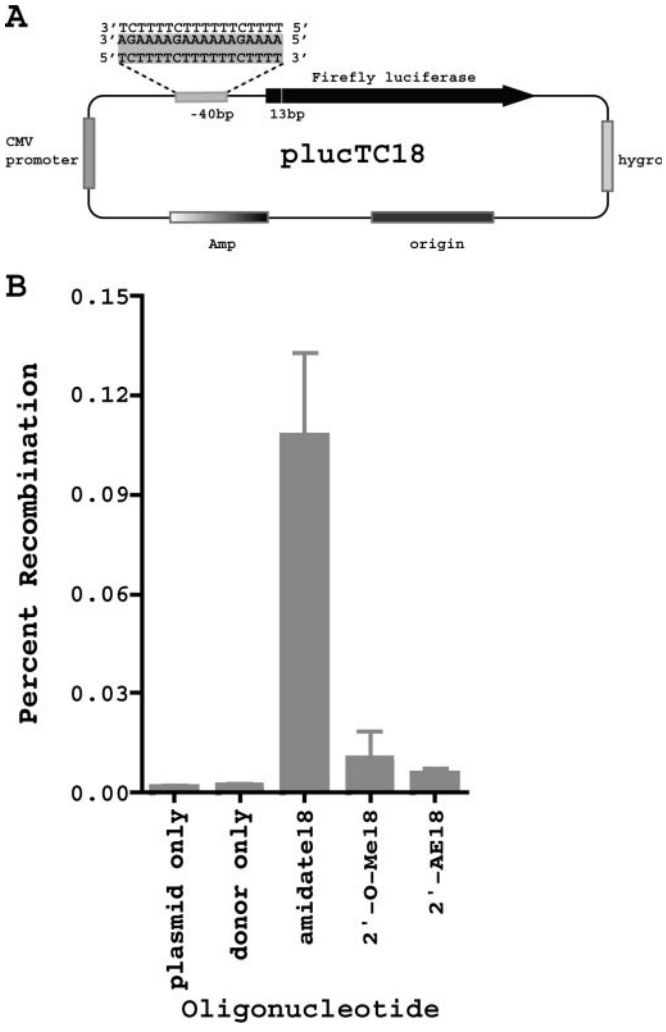

Figure 5. Intermolecular induced recombination mediated by pyrimidine TFOs. (**A**) Schematic representation of the plucTC18 construct. The plasmid contains the pyrimidine triplex binding site located 40 bp upstream of the start codon for the firefly luciferase gene. The luciferase gene has a nonsense mutation at 13 bp downstream from the start codon. (**B**) Percent recombination in CHO cells. Plasmid, TFO, and the donor oligonucleotide (Fluc13) were co-transfected into CHO cells. After 48 h, cells were lysed and recombination was measured based on relative light units and normalized to protein.

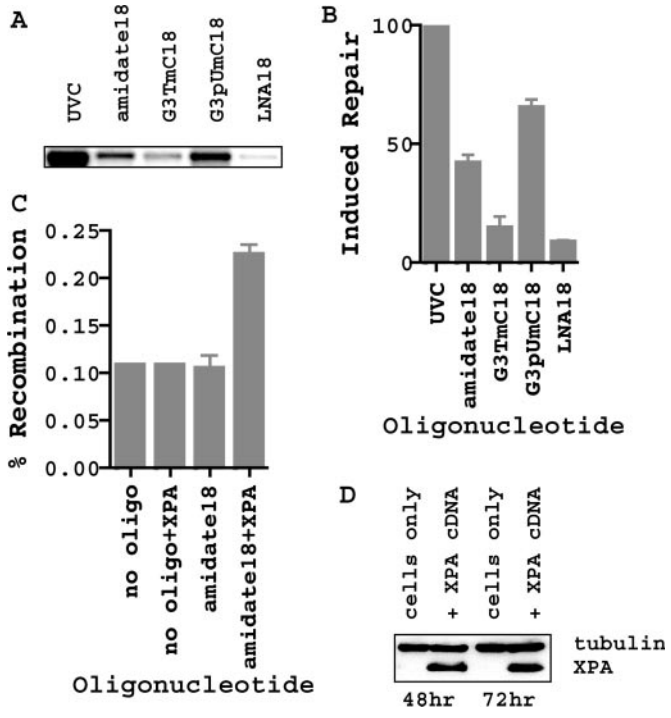

Figure 6. Pyrimidine motif TFOs and DNA repair. (**A**) Pyrimidine triplex-induced DNA repair in HeLa cell extracts. TFOs and plasmids were co-incubated in HeLa cell-free extracts supplemented with [α-^{32}P]dCTP. Induced DNA repair synthesis was measured by visualization and quantification of incorporation of [α-^{32}P]dCTP into the plasmid. As a positive control, plasmid alone was treated with UVC irradiation. (**B**) Quantification of induced repair as measured by [α-^{32}P]dCTP incorporation in (A); normalized to UVC-treated plasmid representing 100% repair activity. (**C**) Dependence of triplex-induced recombination on XPA. XP12BE (XPA-deficient) cells were transfected with the dual supF reporter construct containing the pyrimidine motif triplex binding site and then transfected or not with the amidate18 TFO. Parallel samples were also transfected with XPA cDNA at the same time as the dual supF vector. Induced recombination was assayed as in Figures 3 and 4. (**D**) Levels of XPA expression in XP12BE cells versus XP12BE cells transfected with an XPA cDNA construct. XP12BE cells and XP12BE cells transfected with XPA cDNA were collected at 48 and 72 h post-transfection and expression of XPA was detected by western blot.

assay similar to that used in COS-7 cells, above, was performed in XP12BE cells. These cells are SV40 transformed fibroblasts isolated from a patient lacking the Xeroderma Pigmentosum complementation group A protein (XPA, a recognition protein in the NER pathway). The amidate18 TFO was unable to induce recombination in XP12BE cells (Figure 6C). However, with the expression of XPA cDNA, induced recombination by amidate18 was detected (Figure 6C). The expression of XPA in the cDNA-transfected cells was confirmed by western blot (Figure 6D).

Nuclease resistance of pyrimidine TFOs

To test the possibility that differences in resistance to nucleases of the various TFOs could be responsible for the observed differences in induced recombination frequencies, we tested the stability of selected TFOs in serum. The 5′ end-labeled TFOs were added to FBS and aliquots were removed at time points from 0 to 24 h to measure the quantity of full-length oligonucleotide by gel electrophoresis and autoradiography. After 1 h in serum, most of the chemically modified pyrimidine TFOs were intact, except for the unmodified-TFO DNA18 and the 5meC-modified TFO G3TmC18 (Figure 7). After 3 h, the amidate18, LNA18, 2′-O-Me18, 2′-AE18 and the G-rich TFOs all showed that >50% remained intact. The G3pUmC18 TFO showed that ~36% oligonucleotide was intact at 3 h. By 6 h, only the 2′-AE18 and the amidate18 pyrimidine motif TFOs showed >50% intact; the G3pUmC18 TFO showed ~25% intact. In all cases, <10% of the pyrimidine TFOs tested remained intact at 12 h. Interestingly, two G-rich TFOs, AG30 and AG19, showed higher levels of nuclease resistance, with >50% oligonucleotide remaining intact at 24 h (Figure 7) and persisting at this level even up to 72 h (data not shown). This serum stability shown by the G-rich TFOs may, in part, account for their documented effectiveness for gene targeting *in vivo* following systemic administration in mice (5).

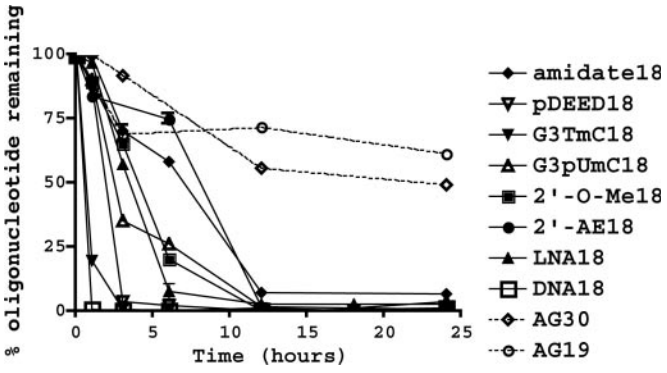

Figure 7. Serum stability of pyrimidine TFOs. [γ-^{32}P]ATP-labeled TFOs were added to FBS and aliquots were removed at time points from 0 to 24 h. The percent oligonucleotide remaining represents the amount of full-length TFO still intact at the given time point.

DISCUSSION

In the work reported here, we tested a series of TFOs with selected chemical modifications for their ability to bind as third strands in the pyrimidine motif under a variety of *in vitro* conditions, for their ability to induce recombination in two different cell-based episomal targeting assays, and for their ability to induce repair in cell extracts. We found that high-affinity *in vitro* binding was necessary but not sufficient for increased intracellular activity. Certain modifications that provide for enhanced *in vitro* binding were only minimally effective at increasing the ability of TFOs to induce recombination in cells or to stimulate repair in cell extracts, while others (amidate18 and G3pUmC18) stood out in the initial screen and their activity held up under close evaluation (showing both high third-strand binding affinity and effective intracellular activity). These differences cannot simply be attributed to differential nuclease resistance.

The modified TFOs with the highest binding affinities under physiological conditions *in vitro* (low Mg^{2+}, high K^+ and neutral pH) were amidate18, G3pUmC18, 2′-AE18 and LNA18. Of these, only the amidate and pdU-modified TFOs mediated increases in recombination frequencies over background, 3.4- and 2.8-fold, respectively. The recombination frequencies in the COS-7 episomal shuttle vector assay produced by amidate18 (0.37%) and G3pUmC18 (0.31%) are comparable with the recombination frequency induced by AG30 in a similar shuttle vector assay (0.40%). These recombination frequencies are based on targeting an episomal, not a chromosomal, target. Transfection of the episomal target 24 h before the oligonucleotide transfection allowed for chromatin assembly on the target plasmid (48). In the purine motif, similar mutagenesis and recombination frequencies have been established in episomal and chromosomal targets using G-rich TFOs with both targets (4,6,17,49).

Using a second episomal targeting assay based on intermolecular recombination in a luciferase reporter gene, similar results were seen with the amidate18 TFO, with a recombination frequency of 0.11% (which is a 48-fold induction of recombination compared with recombination by donor DNA alone in this assay). Thus, in two distinct episomal targeting systems in cells, the amidate18 TFO was seen to induce recombination in the absence of covalent adduct formation.

Additionally, the amidate18 and the G3pUmC18 TFOs induced repair in cell extracts. In cells, the induction of recombination in the shuttle vector assay by amidate18 was found to be dependent on XPA, consistent with the *in vitro* repair results and further suggesting that triplexes formed by amidate18 induce recombination in a repair-dependent manner.

Hence, while several of the chemically modified TFOs in the pyrimidine motif were found to bind well as third strands under physiological conditions *in vitro*, only the amidate18 and G3pUmC18 TFOs were seen to induce recombination and repair. One explanation consistent with our results would be that the triplexes formed by the 2′-AE and LNA-modified TFOs are less effective at provoking DNA repair and thereby less effective at inducing recombination. Our prior work with purine motif TFOs indicated that triplexes can be recognized as 'lesions' in the DNA by factors in the NER pathway, leading to induced repair and recombination (4,20,27). Our current results suggest that the same is true for the pyrimidine motif triplexes formed by amidate18 or G3pUmC18 TFOs.

Conceptually, this recognition is likely to result from helical alterations caused by triplex formation (50). Interestingly, Asensio *et al.* (22) found in an NMR-based structural analysis of pyrimidine motif triplexes that the degree of duplex helical distortion can be influenced by substitutions at the 2′-position of the ribose on the TFO. Comparing TFOs with 2′-deoxy (DNA), 2′-OH (RNA) and 2′-O-methyl (2′-O-Me) ribose moieties, they found that the relative degrees of distortion were DNA > RNA > 2′-O-Me. Hence, RNA-like substitution at the 2′-position in the TFO, which tends to promote a C3-*endo* sugar conformation (51), appears to reduce the helical distortion that occurs upon third-strand binding.

The TFOs showing the highest levels of induced recombination were amidate18 and G3pUmC18 in the pyrimidine motif and AG30 in the purine motif. All of these contain DNA-like deoxyribose. In contrast, the 2′-AE18 and LNA18 TFOs have RNA-like 2′-substituted sugars. In fact, the LNA 2′-substitution (consisting of the 2′-O, 4′-C-methylene bridge) locks the ribose into the RNA-like C3-*endo* conformation (52). This is proposed to be an advantage for triplex formation because it may serve to pre-organize the TFO into a uniform conformation favorable to third-strand binding (52), but it may also serve to minimize the resulting helical distortion. Therefore, based on this model, it is possible that the amidate18, G3pUmC18 and AG30 TFOs may create triplexes that are more distorting than those produced by the 2′-AE18 and LNA18, resulting in an increased ability of the resulting triplexes to provoke DNA repair (as shown) and thereby stimulate recombination.

In conclusion, the work reported here demonstrates that non-covalent pyrimidine TFOs, when appropriately modified, can mediate high-affinity binding, induction of recombination in cells and induction of repair in cell extracts, at levels similar to those seen with G-rich purine TFOs at their respective target sites. These results expand the number of possible reagents for targeted genome modification.

ACKNOWLEDGEMENTS

We thank R. Alam and C. Greaves for oligonucleotide synthesis. We also thank F. Rogers, K. Kim, J. Lloyd, D. Hegan,

L. Cabral, K. Bernstein and Y. Schur for insightful conversations. This work was supported by grants to P.M.G. from NIH (R01CA64186 and R01GM54731), to J.M.K. from NIH Medical Scientist Training Program Grant (GM07205) and to D.L.W. from Cystic Fibrosis and Gene Therapy Center at the University of Iowa and from NIH (P50HL062178). Funding to pay the Open Access publication charges for this article was provided by the Department of Therapeutic Radiology, Yale University School of Medicine.

Conflict of interest statement. None declared.

REFERENCES

1. Cooney,M., Czernuszewicz,G., Postel,E.H., Flint,S.J. and Hogan,M.E. (1988) Site-specific oligonucleotide binding represses transcription of the human c-myc gene *in vitro*. *Science*, **241**, 456–459.
2. Birg,F., Praseuth,D., Zerial,A., Thuong,N.T., Asseline,U., Le Doan,T. and Helene,C. (1990) Inhibition of simian virus 40 DNA replication in CV-1 cells by an oligodeoxynucleotide covalently linked to an intercalating agent. *Nucleic Acids Res*., **18**, 2901–2908.
3. Faruqi,A.F., Seidman,M.M., Segal,D.J., Carroll,D. and Glazer,P.M. (1996) Recombination induced by triple-helix-targeted DNA damage in mammalian cells. *Mol. Cell. Biol*., **16**, 6820–6828.
4. Faruqi,A.F., Datta,H.J., Carroll,D., Seidman,M.M. and Glazer,P.M. (2000) Triple-helix formation induces recombination in mammalian cells via a nucleotide excision repair-dependent pathway. *Mol. Cell. Biol*., **20**, 990–1000.
5. Vasquez,K.M., Narayanan,L. and Glazer,P.M. (2000) Specific mutations induced by triplex-forming oligonucleotides in mice. *Science*, **290**, 530–533.
6. Wang,G., Levy,D.D., Seidman,M.M. and Glazer,P.M. (1995) Targeted mutagenesis in mammalian cells mediated by intracellular triple helix formation. *Mol. Cell. Biol*., **15**, 1759–1768.
7. Moser,H.E. and Dervan,P.B. (1987) Sequence specific cleavage of double helical DNA by triple helix formation. *Science*, **238**, 645–650.
8. Francois,J.C., Saison-Behmoaras,T. and Helene,C. (1988) Sequence-specific recognition of the major groove of DNA by oligodeoxynucleotides via triple helix formation. Footprinting studies. *Nucleic Acids Res*., **16**, 11431–11440.
9. Letai,A.G., Palladino,M.A., Fromm,E., Rizzo,V. and Fresco,J.R. (1988) Specificity in formation of triple-stranded nucleic acid helical complexes: studies with agarose-linked polyribonucleotide affinity columns. *Biochemistry*, **27**, 9108–9112.
10. Beal,P.A. and Dervan,P.B. (1991) Second structural motif for recognition of DNA by oligonucleotide-directed triple-helix formation. *Science*, **251**, 1360–1363.
11. Knauert,M.P. and Glazer,P.M. (2001) Triplex forming oligonucleotides: sequence-specific tools for gene targeting. *Hum. Mol. Genet*., **10**, 2243–2251.
12. Chan,P.P. and Glazer,P.M. (1997) Triplex DNA: fundamentals, advances, and potential applications for gene therapy. *J. Mol. Med*., **75**, 267–282.
13. Lacroix,L., Lacoste,J., Reddoch,J.F., Mergny,J.L., Levy,D.D., Seidman,M.M., Matteucci,M.D. and Glazer,P.M. (1999) Triplex formation by oligonucleotides containing 5-(1-propynyl)-2′-deoxyuridine: decreased magnesium dependence and improved intracellular gene targeting. *Biochemistry*, **38**, 1893–1901.
14. Puri,N., Majumdar,A., Cuenoud,B., Natt,F., Martin,P., Boyd,A., Miller,P.S. and Seidman,M.M. (2002) Minimum number of 2′-*O*-(2-aminoethyl) residues required for gene knockout activity by triple helix forming oligonucleotides. *Biochemistry*, **41**, 7716–7724.
15. Sachsenmaier,C., Radler-Pohl,A., Zinck,R., Nordheim,A., Herrlich,P. and Rahmsdorf,H.J. (1994) Involvement of growth factor receptors in the mammalian UVC response. *Cell*, **78**, 963–972.
16. Majumdar,A., Khorlin,A., Dyatkina,N., Lin,F.L., Powell,J., Liu,J., Fei,Z., Khripine,Y., Watanabe,K.A., George,J. *et al*. (1998) Targeted gene knockout mediated by triple helix forming oligonucleotides. *Nature Genet*., **20**, 212–214.
17. Vasquez,K.M., Wang,G., Havre,P.A. and Glazer,P.M. (1999) Chromosomal mutations induced by triplex-forming oligonucleotides in mammalian cells. *Nucleic Acids Res*., **27**, 1176–1181.
18. Vasquez,K.M., Dagle,J.M., Weeks,D.L. and Glazer,P.M. (2001) Chromosome targeting at short polypurine sites by cationic triplex-forming oligonucleotides. *J. Biol. Chem*., **276**, 38536–38541.
19. Barre,F.X., Giovannangeli,C., Helene,C. and Harel-Bellan,A. (1999) Covalent crosslinks introduced via a triple helix-forming oligonucleotide coupled to psoralen are inefficiently repaired. *Nucleic Acids Res*., **27**, 743–749.
20. Wang,G. and Glazer,P.M. (1995) Altered repair of targeted psoralen photoadducts in the context of an oligonucleotide-mediated triple helix. *J. Biol. Chem*., **270**, 22595–22601.
21. Faruqi,A.F., Egholm,M. and Glazer,P.M. (1998) Peptide nucleic acid-targeted mutagenesis of a chromosomal gene in mouse cells. *Proc. Natl Acad. Sci. USA*, **95**, 1398–1403.
22. Asensio,J.L., Carr,R., Brown,T. and Lane,A.N. (1999) Conformational and thermodynamic properties of parallel intramolecular triple helices containing a DNA, RNA, or 2′-OMeDNA third strand. *J. Am. Chem. Soc*., **121**, 11063–11070.
23. Parris,C.N. and Seidman,M.M. (1992) A signature element distinguishes sibling and independent mutations in a shuttle vector plasmid. *Gene*, **117**, 1–5.
24. Kraemer,K.H. and Seidman,M.M. (1989) Use of supF, an *Escherichia coli* tyrosine suppressor tRNA gene, as a mutagenic target in shuttle-vector plasmids. *Mutat. Res*., **220**, 61–72.
25. Knauert,M.P., Lloyd,J.A., Rogers,F.A., Datta,H.J., Bennett,M.L., Weeks,D.L. and Glazer,P.M. (2005) Distance and affinity dependence of triplex-induced recombination. *Biochemistry*, **44**, 3856–3864.
26. Bradford,M.M. (1976) A rapid and sensitive method for the quantitation of microgram quantities of protein utilizing the principle of protein-dye binding. *Anal. Biochem*., **72**, 248–254.
27. Datta,H.J., Chan,P.P., Vasquez,K.M., Gupta,R.C. and Glazer,P.M. (2001) Triplex-induced recombination in human cell-free extracts. Dependence on XPA and HsRad51. *J. Biol. Chem*., **276**, 18018–18023.
28. Rogers,F.A., Vasquez,K.M., Egholm,M. and Glazer,P.M. (2002) Site-directed recombination via bifunctional PNA–DNA conjugates. *Proc. Natl Acad. Sci. USA*, **99**, 16695–16700.
29. Gryaznov,S.M., Lloyd,D.H., Chen,J.K., Schultz,R.G., DeDionisio,L.A., Ratmeyer,L. and Wilson,W.D. (1995) Oligonucleotide N3′→P5′ phosphoramidates. *Proc. Natl Acad. Sci. USA*, **92**, 5798–5802.
30. Testa,S.M., Gryaznov,S.M. and Turner,D.H. (1998) Antisense binding enhanced by tertiary interactions: binding of phosphorothioate and N3′→P5′ phosphoramidate hexanucleotides to the catalytic core of a group I ribozyme from the mammalian pathogen *Pneumocystis carinii*. *Biochemistry*, **37**, 9379–9385.
31. Skorski,T., Perrotti,D., Nieborowska-Skorska,M., Gryaznov,S. and Calabretta,B. (1997) Antileukemia effect of c-myc N3′→P5′ phosphoramidate antisense oligonucleotides *in vivo*. *Proc. Natl Acad. Sci. USA*, **94**, 3966–3971.
32. Gryaznov,S., Skorski,T., Cucco,C., Nieborowska-Skorska,M., Chiu,C.Y., Lloyd,D., Chen,J.K., Koziolkiewicz,M. and Calabretta,B. (1996) Oligonucleotide N3′→P5′ phosphoramidates as antisense agents. *Nucleic Acids Res*., **24**, 1508–1514.
33. Giovannangeli,C., Diviacco,S., Labrousse,V., Gryaznov,S., Charneau,P. and Helene,C. (1997) Accessibility of nuclear DNA to triplex-forming oligonucleotides: the integrated HIV-1 provirus as a target. *Proc. Natl Acad. Sci. USA*, **94**, 79–84.
34. Matteucci,M., Lin,K.Y., Huang,T., Wagner,R., Sternbach,D.D., Mehrotra,M. and Besterman,J.M. (1997) Sequence-specific targeting of duplex DNA using a camptothecin-triple helix forming oligonucleotide conjugate and topoisomerase I. *J. Am. Chem. Soc*., **119**, 6939–6940.
35. Fenster,S.D., Wagner,R.W., Froehler,B.C. and Chin,D.J. (1994) Inhibition of human immunodeficiency virus type-1 env expression by C-5 propyne oligonucleotides specific for Rev-response element stem–loop V. *Biochemistry*, **33**, 8391–8398.
36. Wahlestedt,C., Salmi,P., Good,L., Kela,J., Johnsson,T., Hokfelt,T., Broberger,C., Porreca,F., Lai,J., Ren,K. *et al*. (2000) Potent and nontoxic antisense oligonucleotides containing locked nucleic acids. *Proc. Natl Acad. Sci. USA*, **97**, 5633–5638.
37. Torigoe,H., Hari,Y., Sekiguchi,M., Obika,S. and Imanishi,T. (2001) 2′-O,4′-C-methylene bridged nucleic acid modification promotes pyrimidine motif triplex DNA formation at physiological pH: thermodynamic and kinetic studies. *J. Biol. Chem*., **276**, 2354–2360.

38. Arzumanov,A., Walsh,A.P., Rajwanshi,V.K., Kumar,R., Wengel,J. and Gait,M.J. (2001) Inhibition of HIV-1 Tat-dependent trans activation by steric block chimeric 2′-O-methyl/LNA oligoribonucleotides. *Biochemistry*, **40**, 14645–14654.
39. McCaffrey,A.P., Meuse,L., Karimi,M., Contag,C.H. and Kay,M.A. (2003) A potent and specific morpholino antisense inhibitor of hepatitis C translation in mice. *Hepatology*, **38**, 503–508.
40. Lacroix,L., Arimondo,P.B., Takasugi,M., Helene,C. and Mergny,J.L. (2000) Pyrimidine morpholino oligonucleotides form a stable triple helix in the absence of magnesium ions. *Biochem. Biophys. Res. Commun.*, **270**, 363–369.
41. Lee,J.S., Woodsworth,M.L., Latimer,L.J. and Morgan,A.R. (1984) Poly(pyrimidine). poly(purine) synthetic DNAs containing 5-methylcytosine form stable triplexes at neutral pH. *Nucleic Acids Res.*, **12**, 6603–6614.
42. Xodo,L.E., Manzini,G., Quadrifoglio,F., van der Marel,G.A. and van Boom,J.H. (1991) Effect of 5-methylcytosine on the stability of triple-strand DNA—a thermodynamic study. *Nucleic Acids Res.*, **19**, 5625–5631.
43. Vasquez,K.M., Wensel,T.G., Hogan,M.E. and Wilson,J.H. (1995) High-affinity triple helix formation by synthetic oligonucleotides at a site within a selectable mammalian gene. *Biochemistry*, **34**, 7243–7251.
44. Cheng,A.J. and Van Dyke,M.W. (1993) Monovalent cation effects on intermolecular purine–purine–pyrimidine triple-helix formation. *Nucleic Acids Res.*, **21**, 5630–5635.
45. Wang,G., Seidman,M.M. and Glazer,P.M. (1996) Mutagenesis in mammalian cells induced by triple helix formation and transcription-coupled repair. *Science*, **271**, 802–805.
46. Husain,S.I., Carlton,W. and Sancar,A. (1989) Human nucleotide excision repair *in vitro*: repair of pyrimidine dimers, psoralen and cisplatin adducts by HeLa cell-free extract. *Nucleic Acids Res.*, **17**, 4471–4484.
47. Wood,R.D., Robins,P. and Lindahl,T. (1988) Complementation of the xeroderma pigmentosum DNA repair defect in cell-free extracts. *Cell*, **53**, 97–106.
48. Cereghini,S. and Yaniv,M. (1984) Assembly of transfected DNA into chromatin: structural changes in the origin–promoter–enhancer region upon replication. *EMBO J.*, **3**, 1243–1253.
49. Luo,Z., Macris,M.A., Faruqi,A.F. and Glazer,P.M. (2000) High-frequency intrachromosomal gene conversion induced by triplex-forming oligonucleotides microinjected into mouse cells. *Proc. Natl Acad. Sci. USA*, **97**, 9003–9008.
50. Vasquez,K.M., Christensen,J., Li,L., Finch,R.A. and Glazer,P.M. (2002) Human XPA and RPA DNA repair proteins participate in specific recognition of triplex-induced helical distortions. *Proc. Natl Acad. Sci. USA*, **99**, 5848–5853.
51. Holland,J.A. and Hoffman,D.W. (1996) Structural features and stability of an RNA triple helix in solution. *Nucleic Acids Res.*, **24**, 2841–2848.
52. Sun,B.W., Babu,B.R., Sorensen,M.D., Zakrzewska,K., Wengel,J. and Sun,J.S. (2004) Sequence and pH effects of LNA-containing triple helix-forming oligonucleotides: physical chemistry, biochemistry, and modeling studies. *Biochemistry*, **43**, 4160–4169.